Author Manuscript

Author Manuscript

Author Manuscript

Author Manuscript

HHS Public Access

Author manuscript

Int J Cancer. Author manuscript; available in PMC 2019 July 01.

Published in final edited form as:

Int J Cancer. 2018 July 01; 143(1): 113–126. doi:10.1002/ijc.31290.

Arsenic Promotes the COX2/PGE2-SOX2 Axis to Increase the Malignant Stemness Properties of Urothelial Cells

Akira Ooki[1], **Asma Begum**[2], **Luigi Marchionni**[3], **Christopher J. VandenBussche**[4], **Shifeng Mao**[5], **Max Kates**[6], and **Mohammad Obaidul Hoque**[1,3,6,*]

[1]Department of Otolaryngology-Head and Neck Surgery, Johns Hopkins University School of Medicine, Baltimore, Maryland 21231, USA

[2]The Sidney Kimmel Comprehensive Cancer, Johns Hopkins University, Baltimore, Maryland 21231, USA

[3]Department of Oncology, Johns Hopkins University School of Medicine, Baltimore, Maryland 21231, USA

[4]Department of Pathology, Johns Hopkins University School of Medicine, Baltimore, Maryland 21231-2410, USA

[5]Allegheny Health Network Cancer Institute, Pittsburgh, PA 15212, USA

[6]Department of Urology, Johns Hopkins University School of Medicine, Baltimore, Maryland 21287, USA

Abstract

Chronic arsenic exposure is associated with the development of urothelial carcinoma of the bladder (UCB). To elucidate the contribution of arsenic exposure to urothelial cancer stem cell (CSC) generation, we established an *in vitro* stepwise malignant model transformed by chronically exposing human urothelial cells to arsenic. Using this model, we found that chronic arsenic exposure endows urothelial cells with malignant stemness properties including increased expression of stemness-related factors such as SOX2, sphere formation, self-renewal, invasion, and chemo-resistance. SOX2 was gradually and irreversibly overexpressed in line with acquired sphere-forming and self-renewal abilities. Following gene set enrichment analyses of arsenic-exposed and arsenic-unexposed cells, we found COX2 as an enriched gene for oncogenic signature. Mechanistically, arsenic-induced COX2/PGE2 increases SOX2 expression that eventually promotes malignant stem cell generation and repopulation. In urine samples from 90 subjects exposed to arsenic and 91 control subjects, we found a significant linear correlation between SOX2 and COX2 expression and the potential of SOX2 and COX2 expression as urinary markers to detect subjects exposed to arsenic. Furthermore, the combination marker yielded a high sensitivity for UCB detection in a separate cohort. Finally, our *in vitro* model exhibits basal-type molecular features, and dual inhibition of EGFR and COX2 attenuated stem cell enrichment more

*Corresponding author as a Lead Contact: Mohammad Obaidul Hoque, DDS, Ph.D., Department of Otolaryngology and Head & Neck Surgery, The Johns Hopkins University School of Medicine 1550 Orleans Street, CRB II, 5M.07, Baltimore, MD 21231. Phone 410-502-8778; Fax 410-614-1411; mhoque1@jhmi.edu.

Conflict of interest: The authors declare no potential conflicts of interest.

Author Manuscript Author Manuscript Author Manuscript Author Manuscript

efficiently than an EGFR inhibitor alone. In conclusion, the COX2/PGE2-SOX2 axis promotes arsenic-induced malignant stem cell transformation. In addition, our findings indicate the possible use of SOX2 and COX2 expression as urinary markers for the risk stratification and detection of UCB.

Keywords

urothelial carcinoma of bladder; arsenic; cancer stem cell; SOX2; COX2

Introduction

Arsenic is a common environmental contaminant and a major public health concerns worldwide due to the devastating toxic effects of the metalloid[1,2]. Inorganic arsenic is associated with the development of urothelial carcinoma of the bladder (UCB) in a dose-dependent manner[2,3]. Therefore, UCB tumorigenesis may be better understood through the mechanisms of arsenic-induced UCB initiation and progression. Arsenic-induced cancer animal models have been difficult to develop due to significant species-specific differences in terms of arsenic metabolism and susceptibility to its toxicity[4,5]. Moreover, there is no suitable model to study the stepwise molecular alterations caused by arsenic exposure in UCB. These limitations have hampered the development of appropriate clinical management of UCB, including biomarkers for the early cancer detection and risk assessment for environmental exposure to carcinogens such as arsenic.

UCB follows the cancer stem cell (CSC) model, in which a relatively rare population of cancer cells contributes to cancer initiation and progression driven by their cancer stemness properties including sphere formation, self-renewal, invasion, and differentiation[6]. A large body of evidence suggests that normal stem cells may be the direct target of carcinogens and thus may be the ‘origin of CSCs’[7]. Indeed, chronic arsenic exposure transforms normal stem cells into a CSC phenotype in prostate and renal *in vitro* models[8,9]. However, the association of arsenic exposure with urothelial CSCs and the relevant mechanisms behind arsenic-induced CSCs have yet to be fully elucidated.

Sex-determining region Y [SRY]-box 2 (SOX2) is a prominent transcription factor that promotes pluripotency and self-renewal in embryonic stem cells[10] and generates induced pluripotent stem cells[11]. In several cancer types, SOX2 plays a crucial role in maintaining CSCs, and it establishes a continuum between cancer initiation and progression via the direct regulation of key genes that control cancer stemness, survival, proliferation, and invasion[12,13]. As UCB is an environmental exposure-associated disease and SOX2 is overexpressed in UCB[14], we hypothesized that arsenic exposure might elicit the dysregulation of stemness-related factors such as SOX2 to promote stem cell properties and to initiate and repopulate urothelial CSCs.

Chronic inflammation caused by continuous exposure to chemical carcinogens (such as arsenic) has been linked to carcinogenesis[15]. The inflammatory enzyme cyclooxygenase 2 (COX2) and the COX2-derived prostaglandin E2 (PGE2) pathway plays a key role in promoting the multistep development of cancer, from initiation to metastasis[16]. Chronic

Author Manuscript Author Manuscript Author Manuscript Author Manuscript

arsenic exposure promotes COX2 expression[9,17], which is predominantly expressed in the majority of UCB but not in normal urothelium[18]. A COX2 transgenic mouse model, which shows that COX2 overexpression is sufficient to cause UCB through transitional cell hyperplasia, suggests that COX2 overexpression may be associated with the development of UCB[19]. Furthermore, epidemiological and clinical studies support the chemo-preventive effects of COX2 inhibitors on UCB incidence[20]. Notably, COX2/PGE2 has been shown to play a central role in CSC repopulation[21]. Thus, arsenic exposure may promote the connections among carcinogenesis, chronic inflammation, and CSC generation through COX2/PGE2 signaling. However, it remains unclear how arsenic-induced COX2/PGE2 signaling promotes CSC traits.

We recently developed an *in vitro* stepwise malignant model transformed by chronically exposing human urothelial HUC1 cells to arsenic[22]. Using this model, we reveal that arsenic-induced COX2/PGE2 signaling increases SOX2 expression that promotes malignant stem cell transformation. In addition, the expression levels of urinary SOX2 and COX2 have the potential of non-invasive biomarkers for risk assessment of arsenic exposure and for UCB detection. Furthermore, COX2 inhibition may suppress CSC enrichment following epidermal growth factor receptor (EGFR)-targeted therapy in this basal-type molecular features exhibiting *in vitro* model.

Materials and Methods

Compounds and reagents

Arsenic trioxide (AS_2O_3) and COX2 selective inhibitor celecoxib were purchased from Sigma-Aldrich (St. Louis, USA). Prostaglandin E2 (PGE2) was purchased from Cayman Chemical (Ann Arbor, USA). EGFR small molecule inhibitor erlotinib was purchased from BioVision (Milpitas, USA). PGE2 receptor 4 (EP4) antagonist ONO-AE3-208, EP3 antagonist L-798,106, EP1 and EP2 antagonist AH 6809, and COX2 selective inhibitor etodolac were purchased from Tocris Bioscience (Ellisville, USA).

Cell lines and tissue samples

SV-40 immortalized human urothelial cell line (HUC1) was obtained from the American Type Culture Collection. BFTC 905 and BFTC 909 cell lines were established from arsenic-exposed urothelial carcinoma subjects[23] and obtained from the German Collection of Microorganisms and Cell Cultures (Braunschweig). Re-authentification of cells was performed using PowerPlex 16 HS for short tandem repeats analysis at the Johns Hopkins University School of Medicine (JHUSOM), Institute of Genetic Medicine core facility, and all cell lines have been confirmed as authentic. To prepare the *in vitro* arsenic model, we chronically exposed HUC1 cells to 1μM arsenic trioxide, as described previously[22], and arsenic-exposed (As) cells and passage-matched arsenic unexposed control (UE) cells were stock for each months until 12 months. To determine the arsenic withdrawal effect, we cultured cells exposed to arsenic for 10 months (10M As) and 12 months (12M As) without arsenic for 2.5 months (10M As+2.5M UE and 12M As+2.5M UE-cells).

Author Manuscript Author Manuscript Author Manuscript Author Manuscript

Ninety urine samples from non-cancer subjects exposed to arsenic were collected from the Health Effects of Arsenic Longitudinal Study (HEALS) cohort, an ongoing population-based prospective cohort study in Araihazar, Bangladesh[24] and kindly provided by Dr. Habibul Ahsan, The University of Chicago, Chicago, Illinois. The levels of arsenic in drinking water in Araihazar range from 0.1 μg/L to >100 μg/L. The arsenic exposure status of subjects was determined through drinking water arsenic concentrations measured in the subject's primary tube-well used for water consumption. The concentrations of arsenic in drinking water >10 μg/L were considered high As-exposure because exposure to 10 μg/L of arsenic in drinking water is maximum acceptable arsenic concentration according to the World Health Organization (WHO)[25] and may double the risk of UCB[3]. To confirm the arsenic-exposure–specific alterations, we also tested 91 urine samples collected from the Baltimore area with safe levels of arsenic[22]. Fifty-five urine samples from subjects with UCB were kindly provided from the Johns Hopkins University urine bank. As a control, 108 population-matched urine samples from patients with no history of genitourinary malignancy were obtained from the urine bank. All urinary specimens had confirmed diagnoses by board-certified cytopathologists. Detailed information of the urine sample including subjects with arsenic exposure and UCB is provided in Supplementary Table S1. Informed consent was obtained from the patients before sample collection. Approval to conduct research on human subjects was obtained from the JHUSOM institutional review boards. This study qualified for exemption under the U.S. Department of Health and Human Services policy for protection of human subjects [45 CFR 46.101(b)].

Gene expression profiling

Expression profiles of arsenic-induced malignant transformed HUC1 cells and BFTC905 cells were previously performed using the HumanHT-12 v4 Expression BeadChip (Illumina)[26]. Gene Set Enrichment Analysis (GSEA) was used to identify gene sets enriched by arsenic exposure in oncogenic signatures from the Molecular Signatures Database (MSigDB; Broad Institute). The gene expression data are deposited in the NCBI Gene Expression Omnibus (GEO) database under accession ID GSE90023.

RNA extraction and quantitative reverse transcriptase polymerase chain reaction (Q-RT-PCR)

Total RNA from cell lines was isolated using the RNeasy Plus Mini kit (Qiagen, Valencia, USA) according to the manufacturer's protocol. Urine sample was centrifuged for 5 min at 1500 rpm and the supernatant was used for RNA extraction as described previously[22]. Total RNA extraction from urine was performed using the MirVana miRNA Isolation Kit (Ambion, Austin, USA). Q-RT-PCR was performed using the Fast SYBR Green Master Mix (Thermo Fisher Scientific, Waltham, USA) on a 7900HT Fast Real-Time PCR System (Life technologies, Carlsbad, USA) in triplicate. Primer sequences and the thermal cycling conditions were shown in Supplementary Table S2. SDS software (Applied Biosystems) was used to determine cycle threshold (Ct) values. Expression level was quantified relative to β-actin using the 2-ΔΔCt method.

Author Manuscript Author Manuscript Author Manuscript Author Manuscript

Western blotting analysis

Whole cell lysates were extracted using the RIPA buffer (Thermo Scientific) supplemented with 10 μL/mL of the Halt™ Protease Inhibitor Cocktail Kit (Life Technologies) and 30 μL/mL of the Halt™ Phosphatase Inhibitor Cocktail Kit (Life Technologies). COX2 (D5H5), NANOG (D73G4), OCT4 (D7O5Z), CD133 (A3G6K), Snail (C15D3), ZEB1 (D80D3), Vimentin (D21H3), N-cadherin (D4R1H), E-cadheerin (24E10), p-EGFR (D7A5), EGFR (D38B1), p-AKT (D9E), AKT (cat #, 9272), p-ERK (D13.14.4E), ERK (137F5), STAT3 (cat #, 124H6)), p-STAT3 (D3A7), NF-κB (C22B4), and HIF1α (cat #, 3716) antibodies were obtained from Cell Signaling Technology (Danvers, MA, USA), except for SOX2 (EPR3131; Abcam, Cambridge, USA), CD24 (cat #, AF5247-SP; R&D Systems, Minneapolis USA) and β-actin (A2228; Sigma-Aldrich). Secondary horseradish peroxidase (HRP)–conjugated antibodies were obtained from Cell Signaling Technology, and chemiluminescent detection of HRP-labeled antibodies was performed using Amersham ECL Prime Western Blotting Detection Reagent (GE Healthcare, Piscataway, USA). As loading control, β-actin was used.

Enzyme-Linked Immunosorbent Assay (ELISA)

The PGE2 level in cell culture supernatants after erlotinib treatment for 72 hours was measured using quantitative ELISA kits (R&D Systems).

Gene silencing and expression

SOX2 shRNA pGFP-C-shLenti Vector (SOX2-sh) was used for the knockdown of the gene expression (Origene, Rockville, USA). Non-effective 29-mer scrambled shRNA pGFP-C-shLenti Vector (Origene) was used as a control (SOX2-Ctrl). EF1A-Human-SOX2 lentivirus (SOX2-LV) for SOX2 induction was purchased from Cellomics Technology (Rockville, USA). EF1A-vector control lentivirus was used as a control. For the knockdown of COX2, COX-2 Silencer Select siRNA (Thermo Fisher Scientific) was used.

Sphere formation assay and self-renewal assay

Sphere formation was performed by culturing cells (2×10^4/well) in DMEM/Ham's F12 50/50 Mix (Mediatech) supplemented with B-27 (Life Technologies), 20 ng/mL the fibroblast growth factors (FGF)-basic (Peprotech, New Jersey, USA), 20 ng/mL epidermal growth factor (EGF) (Peprotech). Cell culture was performed in ultra-low attachment 6 well plates (Corning, Lowell, USA) for 14 days. The medium was replaced every other day. Sphere formation was evaluated using the inverted phase-contrast microscope, and single sphere with a diameter larger than 100 μm was counted using NIS-Elements Microscope Imaging Software (Nikon Instruments). To re-differentiate spheres, we plated spheres in standard growth medium with 10% fetal bovine serum (FBS) in dishes supporting cell attachment, and incubated for 7 days.

For self-renewal assay, primary spheres were collected by gentle centrifugation (5 min at 400 × g), dissociated with Stempro Accutase Cell Dissociation Reagent (Life Technologies), and mechanically disrupted with a pipette. The cell suspension was sieved through 40μm cell strainer cap filter to achieve a single-cell suspension, and then equal numbers of alive

Author Manuscript Author Manuscript Author Manuscript Author Manuscript

cells were plated in ultralow attachment plates to generate the second spheres. All the experiments were performed in triplicate and repeated at least three times.

Cell proliferation and viability assay (MTT assay)

The cell proliferative and viability activity were measured using the 3-(4, 5-dimethyl thiazol-2-yl)-2, 5-diphenyltetrazolium bromide (MTT) Proliferation Assay Kit (ATCC; Manassas, VA, USA) according to the manufacturer's protocol. Spheroid cells were cultured in ultra-low attachment 96 well plates under serum-free condition. Cell viability was expressed as the ratio of absorbance values of the treated cells related to the untreated control cells considered as 1.0. The half maximal (50%) inhibitory concentration (IC_{50}) value of drug was calculated by treatment with the various concentration for 72 hours using MTT assay. Each assay was performed in triplicate, and each experiment was repeated at least three times.

Invasion assay and wound healing assay

The invasion assay was performed using the 24-well BD BioCoat Matrigel Invasion Chamber (BD Biosciences, San Jose, USA) according to the manufacturer’s protocol. Cells that had invaded through the membrane were counted under a microscope in 10 randomly selected fields (magnification ×20) per well and averaged.

The wound healing assay was performed using the Culture-Inserts (ibidi, Verona, USA). The area of wound coverage was calculated using NIS-Elements Microscope Imaging Software.

Apoptosis assay

For apoptosis assay, cells were exposed to erlotinib (1 μM) for 72 hours under serum-free medium and stained with PE Annexin V and 7-AAD for discrimination of early and late apoptosis using the PE Annexin V Apoptosis Detection Kit I (BD Biosciences).

Statistical analysis

In each set of data analyses, the estimate variation is indicated in each figure as a standard error of mean (SEM). The two groups were compared with the Wilcoxon–Mann–Whitney test. A comparison between the multiple groups was performed using the Kruskal–Wallis with post-hoc test (Dwass-Steel test) for non-parametrically continuous variables. The level of statistical significance was set at $P < 0.05$. All statistical analyses were conducted using the JMP 12 software package (SAS Institute).

Results

Chronic arsenic exposure induces malignant stem cells

Using an *in vitro* stepwise model, we previously showed that the chronic exposure of human urothelial HUC1 cells to arsenic (As-cells) for 8 months induced a malignant transformation characterized by increased invasiveness and non-adherent growth in soft agar compared with the passage-matched arsenic unexposed (UE) control cells[22]. To further induce malignant phenotype, we extended the period of arsenic exposure to 12 months. Consistent with a previous report[8], cells exposed to arsenic for 12 months (12M As-cells) showed more

Author Manuscript Author Manuscript Author Manuscript Author Manuscript

tolerance to acute arsenic toxicants, along with a higher innate expression of arsenic-adaptive molecules, such as arsenic efflux, protection from arsenic-induced apoptosis, and oxidative damage (Supplementary Fig. S1A–B). Furthermore, a longer period of arsenic exposure irreversibly endowed urothelial cells with more aggressive properties, including enhanced proliferation, migration and invasion (Supplementary Fig. S1C–E). In our model, As-cells gained a survival selection advantage against the arsenic toxicant, which may result in the accumulation of the molecular alterations necessary for a malignant transformation.

Because chronic arsenic exposure has been shown to affect normal stem cell dynamics and differentiation, leading to an overabundance of CSCs[9], we carried out functional and comprehensive molecular analyses of As-cells to assess the contribution of arsenic to urothelial CSC generation and expansion. As-cells formed significantly more spheres than UE-cells from 10 months of arsenic exposure, and the number of spheres was increased through two subsequent serial passages, indicating arsenic-induced sphere-forming and self-renewal abilities (Fig. 1A). Moreover, these abilities were enhanced dramatically with a prolonged duration of arsenic exposure. To reveal the molecules responsible for arsenic-induced malignant stemness properties, we tested the expression of a panel of stemness-related molecules in 12M UE, 12M As-, and spheroid cells derived from 12M As-cells (spheroid 12M As-cells). As expected, numerous stemness-related molecules, including SOX2, OCT4, NANOG, CD133, and CD24, were upregulated in spheroid cells. Among these molecules, SOX2 showed the most elevated alteration in parental As-cells as well as in spheroid As-cells compared with UE-cells (Fig. 1B). Of note, SOX2 was overexpressed gradually and irreversibly in line with the spheroid-forming and self-renewal abilities acquired from 10 months of arsenic exposure (Supplementary Fig. S2). We confirmed the overexpression of these stemness-related molecules at the protein levels in both parental and spheroid As-cells (Fig. 1C, **left panel**). In addition, the epithelial-mesenchymal transition (EMT) program facilitates CSC generation and expansion[27] and our previous work demonstrated that chronic arsenic exposure induced EMT-like morphologic changes[22]. Indeed, increased expression of mesenchymal markers (N-cadherin and Vimentin) and decreased expression of the epithelial marker (E-cadherin) were observed in As-cells, especially spheroid As-cells (Fig. 1C, **right panel**), indicating the arsenic-induced EMT.

Spheres reflect the potential to exhibit stem cell traits when cells are removed from their microenvironmental niche. Therefore spheroid cells contain enriched stem cell populations[28]. Indeed, when spheres were cultured under standard conditions containing FBS, the globular and floating spheres attached to the culture dish and recapitulated parental cell morphology. In addition, the attached cells showed higher expression of the differentiation markers uroplakin II and IIIa[6] and lower expression of stemness-related molecules than the corresponding spheroid cells, indicating a re-differentiated phenotype (Fig. 1D). To determine whether spheroid As-cells possessed a chemo-resistant phenotype, spheroid As-cells and spheroid UE-cells were treated with various concentrations of cisplatin (CDDP) and gemcitabine (GEM) for 72 hours. As determined by the MTT assay, cell survival was significantly greater in spheroid 12M As-cells compared with spheroid 12M UE-cells, whereas re-differentiated cells were more sensitive to chemotherapy than spheroid cells (Fig 1E, **left panel**). Similar results were observed for 10M As-cells and UCB

Author Manuscript Author Manuscript Author Manuscript Author Manuscript

cell lines (BTFC 909 and BFTC 905) established from arsenic exposed subjects, but not for 6M As-cells (Fig 1E, **right panel**). In addition, spheroid As-cells exhibited a more invasive phenotype than spheroid UE-cells (Fig. 1F). Taken together, our findings suggest that chronic arsenic exposure initiates malignant stem cells through the concurrent expression of stemness-related molecules (such as SOX2, OCT4, NANOG, CD133, and CD24) and induction of EMT.

SOX2 is a critical oncogene linked to arsenic-induced malignant stemness properties

To determine the functional role of SOX2 in arsenic-induced malignant stem cells, we employed a lentiviral-based stable knockdown of SOX2 (SOX2-sh) in 12 M spheroid As-cells. Interestingly, SOX2 knockdown lead to the downregulation of OCT4, NANOG, CD133 and CD24 (Fig. 2A). Consistently, SOX2-sh cells showed a lesser sphere-forming ability than the control (SOX2-Ctrl) cells (Fig. 2B). Of note, spheroid SOX2-sh cells no longer exhibited functions comparable to the spheroid SOX2-Ctrl cells in terms of stemness properties, such as invasion and chemo-resistance (Fig. 2C–D). In addition, SOX2 knockdown significantly attenuated an anti-apoptotic ability against CDDP treatment in spheroid cells (Fig. 2E). Thus, SOX2 is an indispensable factor of arsenic-induced malignant stemness properties.

COX2/PGE2 regulates SOX2 expression in arsenic-induced malignant stem cells

To elucidate the relevant molecular alteration in the multistep process of arsenic-induced malignant transformation, we previously performed gene expression profiling and gene set enrichment analyses (GSEA) of UE-cells, As-cells, and BFTC 905 cells to evaluate the sequence of carcinogenic alterations leading to arsenic-induced urothelial cancer[26]. Among the oncogenic signatures enriched by arsenic exposure, PTGS2 (encoding COX2) was one of the top 50 genes with the most enriched score (Fig. 3A and Supplementary Table S3). We confirmed the upregulation of COX2 in As-cells compared with UE-cells by Q-RT-PCR analyses (Supplementary Fig. S3A) and western blotting (Fig. 3B, **upper panel**). In addition, we observed the upregulation of NF-κB, p-STAT3, and HIF1α, the main transcription factors regulating COX2/PGE2 expression[29]. Although SOX2 expression is frequent in UCB[14], amplification is only 4% (18 of 413 cases) in The Cancer Genome Atlas (TCGA) database (http://cancergenome.nih.gov/). Therefore, SOX2 amplification does not appear to be major mechanism for SOX2 overexpression in UCB. Like SOX2 expression, enhanced COX2 expression was observed in spheroid As-cells compared with parental As-cells (Fig. 3B, **upper panel**). To test the link between COX2/PGE2 and SOX2 in arsenic-induced malignant stem cells, we pharmacologically inhibited COX2 in 12M As-cells and 12M As+2.5M UE cells using the COX2 selective inhibitor, celecoxib. The treatment with the COX2 inhibitor resulted in a concentration-dependent reduction of SOX2 expression, and the addition of PGE2 restored SOX2 expression (Fig. 3B, **lower panel**). Furthermore, the inhibition of COX2 significantly reduced the number of spheres, while PGE2 promoted sphere formation even in the presence of celecoxib (Fig. 3C). Since PGE2 receptors (EP1, EP2, EP3, and EP4) have been considered alternative pharmacological targets to the COX2 inhibitor[30], we also tested the effect of the PGE2 receptors antagonists as well as another COX2 inhibitor, etodolac. The EP4-specific antagonist (ONO AE3 208) and etodolac treatment resulted in reduction of SOX2 expression and sphere formation (Supplementary

Author Manuscript Author Manuscript Author Manuscript Author Manuscript

Fig. S3B–C). Thus, our findings suggest that arsenic-induced COX2/PGE2 signaling regulates SOX2 expression and malignant stemness properties and that EP4 may be a key downstream receptor of COX2/PGE2 signaling for SOX2 regulation.

To further confirm the role of COX2/PGE2 in arsenic-induced malignant stemness properties, we transduced SOX2 in COX2 knockdown As-cells. As expected, the genetic knockdown of COX2 resulted in reduced expression of SOX2 and its related molecules, such as OCT4 and NANOG (Fig. 3D), and less number of sphere formation (Fig. 3E). Furthermore, the forced expression of SOX2 in COX2 knockdown As-cells rescued the COX2-attenuated expression of SOX2-related molecules and the sphere-forming ability. In contrast, SOX2 knockdown attenuated PGE2-accelerated stemness properties (Fig. 3F–G), strengthening the influence of COX2/PGE2-SOX2 axis in maintaining malignant stem cells.

Elevated expression of SOX2 and COX2 in urine samples from subjects with arsenic exposure and UCB

Given that urine is the primary route for the elimination of arsenic[31] and the elevated expression of SOX2 and COX2 due to chronic arsenic exposure in our model, we examined the mRNA expression levels of SOX2 and COX2 using urine samples from 91 arsenic-exposed non-cancer subjects and 90 arsenic-unexposed subjects (Supplementary Table S1). The optimal cutoff value for distinguishing expression of SOX2 and COX2 between subjects with or without arsenic exposure was calculated using a receiver operating characteristic (ROC) analysis (Supplementary Fig. S4A). By using the optimal cutoff value for SOX2, the sensitivity and specificity for the detection of subjects exposed to arsenic were 75.6% (68/90) and 80.3% (74/91), respectively, indicating a close association between arsenic exposure and SOX2 expression. The expression levels of SOX2 were significantly higher in arsenic-exposed subjects than in unexposed subjects (Fig. 4A). Although we did not find any statistically significant difference of COX2 expression between subjects with or without arsenic exposure, the expression levels were significantly higher in subjects exposed to a high arsenic concentration (over 10 μg/L of arsenic in drinking water) compared with subjects exposed to a low arsenic concentration (Supplementary Fig. S4B). In addition, a positive linear correlation between SOX2 and COX2 expression was observed in arsenic-exposed subjects, supporting a link between SOX2 and COX2 in arsenic exposure (Fig. 4B, **left**).

Next, we assessed the potential of SOX2 and COX2 for non-invasive cancer detection using urine samples from 55 UCB subjects and 108 population-matched control subjects. The expression levels of SOX2 and COX2 were significantly higher in UCB subjects than in controls (Fig. 4A), and a significant linear correlation was observed between SOX2 and COX2 expression in UCB subjects (Fig. 4B, **right**). Interestingly, SOX2 and COX2 showed significantly increased expression levels in urine samples from UCB subjects compared with those from subjects exposed to arsenic. By determining the optimal cutoff considering maximum sensitivity and specificity using ROC curves, the sensitivity and specificity for cancer detection were 65.5% (36/55) and 82.4% (89/108) for SOX2 and 81.8% (45/55) and 88.9% (96/108) for COX2, respectively (Fig. 4C). When both SOX2 and COX2 were concomitantly evaluated, the sensitivity and specificity were 85.5% (47/55) and 71.3%

Author Manuscript Author Manuscript Author Manuscript Author Manuscript

(77/108), respectively. Of note, the combination of SOX2 and COX2 detected non-muscle invasive bladder cancer (NMIBC) with a sensitivity of 85.0% (34/40) and low-grade UCB with a sensitivity of 92.9% (13/14) (Supplementary Table S4). Strikingly, we were able to detect cytology negative UCB by combination of these two markers with a sensitivity of 75% (12/16).

The COX2 inhibitor represses stem cell expansion following EGFR-targeted therapy in As-cells that exhibit a basal-type signature

Muscle-invasive UCB can be stratified into basal, luminal, and p53-like types based on unique molecular and clinical features[32]. Basal-type UCB is an aggressive phenotype due to its enhanced urothelial CSC traits and EMT features[32,33]. To test whether As-cells exhibit a basal-type signature, we compared the gene expression data of As-cells with an expression profile curated from four different data sets of UCB, including those from the TCGA and MD Anderson Cancer Center databases[32–35] (Supplementary Table S5). We identified the upregulation of basal-type markers, including KRT5 and KRT6, but not non-basal markers, such as FOXA1, GATA3, and KRT 20, in As-cells compared with UE-cells (Fig. 5A). The array-based results were confirmed by Q-RT-PCR (Supplementary Fig. S5). Thus, chronic arsenic exposure induced a basal-type molecular signature in our model.

EGFR has been demonstrated as a potential therapeutic target because of the activated EGFR pathway in basal-type UCB[34,36]. Indeed, we observed activation of EGFR and its downstream AKT and ERK signaling in As-cells (Fig. 5B). Furthermore, we determined increased efficacy of EGFR-targeted therapy (erlotinib) in As-cells compared with UE-cells, while the treatment enriched number of spheres (Fig. 5C). Intriguingly, we found upregulation of COX2 expression following EGFR-targeted therapy and a dramatic reduction of SOX2 expression due to the addition of the COX2 inhibitor (Fig. 5D). Since COX2-derived PGE2 released from apoptotic cells triggers CSC expansion[37], we assessed whether EGFR-targeted therapy promotes apoptosis and subsequent PGE2 production in As-cells. As expected, EGFR-targeted therapy resulted in a significant increase in apoptosis and PGE2 production, while the addition of the COX2 inhibitor attenuated the release of PGE2 from apoptotic cells (Fig. 5E). Furthermore, the COX2 inhibitor prevented the emergence of stem cell expansion following EGFR-targeted therapy (Fig. 5F). Collectively, the COX2/PGE2-SOX2 axis may play a determinant role in CSC enrichment following EGFR-targeted therapy in As-cells that exhibit a basal-type signature.

Discussion

Chronic arsenic exposure not only promotes the malignant transformation of non-cancer cells, but also confers CSC traits[8,9,22]. Emerging evidences indicate the central role of CSCs at the top of the cellular hierarchy in tumor initiation, progression, therapeutic resistance, and metastasis[38]. Therefore, a better understanding of the molecular mechanisms of arsenic-induced urothelial CSC generation and expansion may shed light on the development of novel therapeutic strategies and biomarkers for risk assessment and UCB detection. Here, we show that chronic arsenic exposure promotes SOX2 expression via COX2/PGE2 signaling, endowing urothelial cells with malignant stem cell properties. In addition, we are

Author Manuscript Author Manuscript Author Manuscript Author Manuscript

also reporting for the first time that the expression of SOX2 and COX2 in urine has the potential to detect high-risk subjects exposed to arsenic and UCB subjects as a non-invasive procedure. Finally, using our *in vitro* model that exhibit basal-type molecular features, we determined that COX2 inhibition might suppress CSC enrichment following EGFR-targeted therapy for basal-type UCB.

SOX2 has been implicated in maintaining malignant stemness properties as an oncogene in several types of cancer[1213], whereas it acts as a tumor suppressor by modulating Wnt-related and intestinal genes in gastric cancer[39], indicating the context-dependent behavior of SOX2. Although chronic arsenic exposure reprograms human bronchial epithelial cells to CSCs with SOX2 expression[40], functional role of SOX2 remains unclear in arsenic-induced CSCs. Using an *in vitro* stepwise arsenic model for urothelial malignant transformation, we demonstrate that SOX2 is a critical oncogene associated with arsenic-induced malignant stemness properties. In addition, SOX2 regulated the expressions of various stemness-related molecules, such as OCT4 and NANOG. Indeed, SOX2 regulates two key transcription factors (OCT4 and NANOG) essential to maintaining CSCs[6]. Moreover, SOX2 stabilized the pluripotent state by maintaining OCT4 expression[10]. Thus, SOX2 may act as a master regulator to maintain arsenic-induced CSCs.

An arsenic-induced inflammatory state has been linked to UCB development[15]. The COX2/PGE2 pathway is one of the major hallmarks in tumor-promoting inflammation[16,19]. Two pathways connect cancer and inflammation: an extrinsic pathway driven by inflammatory conditions due to carcinogen exposure and an intrinsic pathway driven by genetic alterations[29]. The two pathways coordinately activate transcription factors, mainly NF-κB, STAT3, and HIF1α, in tumor cells, resulting in the production of inflammatory mediators including COX2/PGE2. In our model, we found that arsenic exposure promoted the expression of COX2 as well as transcription factors noted above. Although the constitutive expression of COX2 and the sustained biogenesis of PGE2 have been shown to play a central role in CSC generation and maintenance[21], it remains poorly understood how arsenic-induced COX2/PGE2 signaling promotes CSC traits. We demonstrate the COX2/PGE2-SOX2 axis is one of the dominant pathway for arsenic-induced malignant stemness properties.

We observed the increased expression of CSC-related markers, including SOX2, CD24, and CD133, along with EMT markers in As-cells, especially in spheroid As-cells. Given a direct link between the EMT and CSCs[27], it is likely that the arsenic-induced malignant stem cells will uniformly express CSC and EMT markers. However, the spheroid cells are heterogeneous populations in terms of the stemness properties[28], and it is therefore indispensable to use the appropriate makers to isolate subpopulation of stem cells among the spheroid As-cells. We recently reported that $CD24^{+}/CD133^{+}$ cells possess the high stemness properties and expression of SOX2 and COX2 in bladder cancer[26]. These markers may be useful to isolate cells with CSC and EMT traits transformed by chronic arsenic exposure.

Environmental and occupational exposures to arsenic are associated with carcinogenesis including UCB, and high levels of arsenic have been found in groundwater in more than 70 countries across 5 continents, including North America, affecting over 200 million people[25].

Author Manuscript Author Manuscript Author Manuscript Author Manuscript

Therefore, the development of biomarkers for the detection of clinically high-risk subjects who exposed to arsenic is important and may provide tools for screening to detect cancer early. Because urine remains many hours in the bladder prior to its excretion and because urine is the primary route of arsenic excretion[31], the bladder urothelium is exposed to higher concentrations of arsenic. Therefore, urine-based molecular markers may be a reliable and non-invasive approach to develop screening strategies for high-risk subjects exposed to arsenic. In addition, urine-based markers may be used as an alternative or adjunct to standard tests for the initial diagnosis of UCB[41]. We found that SOX2 was significantly overexpressed in arsenic-exposed subjects compared with non-exposed subjects with a high sensitivity and specificity, and that the expression levels of COX2 were higher in subjects exposed to a high arsenic concentration compared with those exposed to a low concentration. In addition, SOX2 and COX2 showed significantly increased expression levels in urine samples from UCB subjects compared with samples from those exposed to arsenic. Thus, the step-by-step elevation of SOX2 and COX2 expression may be a promising biomarker for discriminating between subjects with or without arsenic exposure and between subjects with non-cancer and UCB. These markers can also be used for monitoring arsenic exposed subjects and follow-up of NMIBC patients after transurethral resection of bladder tumor (TURBT). Although a urine cytology is standard test for the diagnosis and surveillance of UCB patients, its sensitivity is relatively low, especially for low-grade and low-stage tumors[42,43]. Of note, the combination of SOX2 and COX2 yielded a high sensitivity for cancer detection not only in urine samples from NMIBC (85.0%) but also for low-grade UCB (92.9%). Most importantly, 75% of negative cytological urine samples from UCB were positive for the combination of SOX and COX2 markers. Therefore, these markers have the potential for clinical use as an ancillary tool to complement a cytological examination. However, as infections or any other inflammatory disease in urinary tract may influence in expression of these markers, extensive validation is needed in a larger, independent cohort including various urologic conditions to assess their clinical utility.

Our *in vitro* model showed activated EGFR signaling and sensitivity to EGFR-targeted therapy with the induction of apoptosis in line with basal-type features[32–34]. However, the effective treatment paradoxically promoted stem cell enrichment through COX2/PGE2 signaling. Apoptosis is a well-recognized cell death mechanism due to cytotoxic therapies; however, apoptotic cells release COX2/PGE2 that stimulates the proliferation of surviving CSCs and ultimately accelerates tumor cell repopulation and treatment failure[37]. Thus, apoptosis may be a double-edged sword, as it initially increases cancer cell death with the subsequent growth stimulation of CSCs via increased COX2/PGE2 expression[44]. In a previous study of lung cancer, SOX2 is a major determinant in EGFR-targeted therapy[45]. We observed that combination of COX2 and EGFR inhibitors dramatically repressed SOX2 expression and spheres formation compared with an EGFR inhibitor alone. These findings suggest that the activated COX2/PGE2-SOX2 signaling pathway contributes to the development of resistance against an EGFR inhibitor when used alone. Although it needs to be validated in other pre-clinical models, our findings suggest that an EGFR inhibitor combined with a COX2 inhibitor may be an effective therapeutic strategy for basal-type UCB.

Author Manuscript Author Manuscript Author Manuscript Author Manuscript

Study limitations include data from *in vitro* analyses using single human urothelial HUC1 cell line, which leads to the possibility of a cell type-specific effect. However, our model showed the activation of EGFR, COX2, and transcription factors (NF-κB, p-STAT3, and HIF1α) for COX2/PGE2 expression, which were reported previously in other arsenic exposed models[9,17,46,47]. Furthermore, we assessed the expression status of SOX2 and COX2 using urine samples from arsenic-exposed non-cancer and UCB subjects. Undoubtedly, further studies are needed to determine whether our findings are generalizable to mechanisms of arsenic-induced urothelial carcinogenesis. For the same reason, we cannot conclude whether chronic arsenic exposure predominantly induces basal-type UCB. We used arsenic trioxide (As_2O_3) to establish the *in vitro* arsenic model. Arsenic exists in organic and inorganic forms in the environment. The inorganic arsenic is the most common and toxic form of human environmental exposure, mainly via the contaminated drinking water[48]. Among inorganic state, the two main forms are sodium arsenite ($NaAsO_2$) and arsenic trioxide (As_2O_3), which have been the most frequently studied on arsenic-induced carcinogenesis because of their oxidative genotoxicity and epigenetic disruption[25]. Thus, As_2O_3-based studies might pave the way to elucidate the precise molecular mechanism of arsenic-induced carcinogenesis. However, this study does not discern the molecular mechanisms of other forms of arsenic. With regard to the clinical utility of SOX2 and COX2 as urinary markers, while promising, these findings cannot be considered conclusive because of relatively small sample size analyzed in this study. Therefore, it needs further validation in a larger sample cohort before clinical implementation.

We did not observe *in vivo* tumor formation after injection of 12 M As-cells in NOD/SCID mice. A longer period of arsenic exposure may be needed for UCB development, which could be a challenge for preparing *in vitro* and *in vivo* models with all the tumorigenic properties. Indeed, chronic cigarette smoke-exposed human bronchial epithelial cells are unable to form tumors in mice; however, these cells can form *in vivo* tumor following the introduction of a single *KRAS* mutation known to be involved in lung cancer initiation[49]. Thus, introducing any UCB-specific key mutated gene in our arsenic model may enhance tumor formation *in vivo*. We recognize that *in vivo* animal models are necessary for developing strategies to prevent cancer in human populations exposed to arsenic. However, the inorganic arsenic exposure does not generally induce UCB in the animal models due to their innate insensitivity to arsenic carcinogenesis compared to humans[4,5], except in selected model systems involving a combined exposure of prenatal arsenic and postnatal diethylstilbestrol[5] and co-administration with another carcinogenic agent[50]. Because arsenic exposure alone did not result in tumors of the bladder even in these selected models, it has proven difficult to elucidate the precise role in carcinogenicity of arsenic as a single agent in the current animal model systems. In addition, the significant differences in biokinetics between humans and rodents also remains as a major gap in terms of inter-species comparisons of arsenic carcinogenicity[4,5]. Thus, our *in vitro* human-originated model may be suitable to replicate arsenic exposure in humans. Therefore, this model provides a proof of concept allowing the study of chronic arsenic exposure in human UCB development.

In summary, we demonstrated that chronic arsenic exposure can induce malignant stem cell transformation via the COX2/PGE2-SOX2 axis. In addition, the expression status of SOX2 and COX2 in urine supernatants can potentially serve as non-invasive molecular markers for

Author Manuscript Author Manuscript Author Manuscript Author Manuscript

risk assessment following arsenic exposure, as well as for the UCB detection. Furthermore, our stepwise model with basal-type molecular features indicated that COX2 inhibition might suppress CSC enrichment following EGFR-targeted therapy. Therefore, our findings may facilitate the development of improved therapeutic strategies and diagnosis in UCB.

Supplementary Material

Refer to Web version on PubMed Central for supplementary material.

Acknowledgments

This work was funded by Flight Attendant Medical Research Institute Young Clinical Scientist Award 052401 YCSA (M.H.), Career Development award from SPORE in Cervical Cancer Grants P50 CA098252 (M.H.), Allegheny Health Network-Johns Hopkins Cancer Research Fund 80039465 (M.H.).

Abbreviations

UCB	urothelial carcinoma of the bladder
CSC	cancer stem cell
As-cells	arsenic-exposed cells
UE-cells	passage-matched arsenic unexposed control cells

References

1. Rao CV, Pal S, Mohammed A, Farooqui M, Doescher MP, Asch AS, Yamada HY. Biological effects and epidemiological consequences of arsenic exposure, and reagents that can ameliorate arsenic damage in vivo. Oncotarget. 2017; 8:57605–21. [PubMed: 28915699]
2. IARC. A Review of Human Carcinogens. C. Metals, Arsenic, Fibres and Dusts. Lyon: International Agency for Research on Cancer; 2012. p. 41-93.
3. Saint-Jacques N, Parker L, Brown P, Dummer TJ. Arsenic in drinking water and urinary tract cancers: a systematic review of 30 years of epidemiological evidence. Environ Health. 2014; 13:44. [PubMed: 24889821]
4. Cohen SM, Ohnishi T, Arnold LL, Le XC. Arsenic-induced bladder cancer in an animal model. Toxicol Appl Pharmacol. 2007; 222:258–63. [PubMed: 17109909]
5. Tokar EJ, Benbrahim-Tallaa L, Ward JM, Lunn R, Sams RL 2nd, Waalkes MP. Cancer in experimental animals exposed to arsenic and arsenic compounds. Crit Rev Toxicol. 2010; 40:912–27. [PubMed: 20812815]
6. Ho PL, Kurtova A, Chan KS. Normal and neoplastic urothelial stem cells: getting to the root of the problem. Nat Rev Urol. 2012; 9:583–94. [PubMed: 22890301]
7. Ochieng J, Nangami GN, Ogunkua O, Miousse IR, Koturbash I, Odero-Marah V, McCawley LJ, Nangia-Makker P, Ahmed N, Luqmani Y, Chen Z, Papagerakis S, et al. The impact of low-dose carcinogens and environmental disruptors on tissue invasion and metastasis. Carcinogenesis. 2015; 36(Suppl 1):S128–59. [PubMed: 26106135]
8. Tokar EJ, Qu W, Liu J, Liu W, Webber MM, Phang JM, Waalkes MP. Arsenic-specific stem cell selection during malignant transformation. J Natl Cancer Inst. 2010; 102:638–49. [PubMed: 20339138]
9. Tokar EJ, Person RJ, Sun Y, Perantoni AO, Waalkes MP. Chronic exposure of renal stem cells to inorganic arsenic induces a cancer phenotype. Chem Res Toxicol. 2013; 26:96–105. [PubMed: 23137061]

Author Manuscript Author Manuscript Author Manuscript Author Manuscript

10. Masui S, Nakatake Y, Toyooka Y, Shimosato D, Yagi R, Takahashi K, Okochi H, Okuda A, Matoba R, Sharov AA, Ko MS, Niwa H. Pluripotency governed by Sox2 via regulation of Oct3/4 expression in mouse embryonic stem cells. Nat Cell Biol. 2007; 9:625–35. [PubMed: 17515932]
11. Takahashi K, Yamanaka S. Induction of pluripotent stem cells from mouse embryonic and adult fibroblast cultures by defined factors. Cell. 2006; 126:663–76. [PubMed: 16904174]
12. Boumahdi S, Driessens G, Lapouge G, Rorive S, Nassar D, Le Mercier M, Delatte B, Caauwe A, Lenglez S, Nkusi E, Brohee S, Salmon I, et al. SOX2 controls tumour initiation and cancer stem-cell functions in squamous-cell carcinoma. Nature. 2014; 511:246–50. [PubMed: 24909994]
13. Bass AJ, Watanabe H, Mermel CH, Yu S, Perner S, Verhaak RG, Kim SY, Wardwell L, Tamayo P, Gat-Viks I, Ramos AH, Woo MS, et al. SOX2 is an amplified lineage-survival oncogene in lung and esophageal squamous cell carcinomas. Nat Genet. 2009; 41:1238–42. [PubMed: 19801978]
14. Ruan J, Wei B, Xu Z, Yang S, Zhou Y, Yu M, Liang J, Jin K, Huang X, Lu P, Cheng H. Predictive value of Sox2 expression in transurethral resection specimens in patients with T1 bladder cancer. Med Oncol. 2013; 30:445. [PubMed: 23307254]
15. Aggarwal BB, Shishodia S, Sandur SK, Pandey MK, Sethi G. Inflammation and cancer: how hot is the link? Biochem Pharmacol. 2006; 72:1605–21. [PubMed: 16889756]
16. Wang D, Dubois RN. Eicosanoids and cancer. Nature reviews Cancer. 2010; 10:181–93. [PubMed: 20168319]
17. Ouyang W, Zhang D, Ma Q, Li J, Huang C. Cyclooxygenase-2 induction by arsenite through the IKKbeta/NFkappaB pathway exerts an antiapoptotic effect in mouse epidermal Cl41 cells. Environ Health Perspect. 2007; 115:513–8. [PubMed: 17450217]
18. Shirahama T. Cyclooxygenase-2 expression is up-regulated in transitional cell carcinoma and its preneoplastic lesions in the human urinary bladder. Clin Cancer Res. 2000; 6:2424–30. [PubMed: 10873095]
19. Klein RD, Van Pelt CS, Sabichi AL, Dela Cerda J, Fischer SM, Furstenberger G, Muller-Decker K. Transitional cell hyperplasia and carcinomas in urinary bladders of transgenic mice with keratin 5 promoter-driven cyclooxygenase-2 overexpression. Cancer Res. 2005; 65:1808–13. [PubMed: 15753378]
20. Daugherty SE, Pfeiffer RM, Sigurdson AJ, Hayes RB, Leitzmann M, Schatzkin A, Hollenbeck AR, Silverman DT. Nonsteroidal antiinflammatory drugs and bladder cancer: a pooled analysis. Am J Epidemiol. 2011; 173:721–30. [PubMed: 21367875]
21. Wang D, Fu L, Sun H, Guo L, DuBois RN. Prostaglandin E2 Promotes Colorectal Cancer Stem Cell Expansion and Metastasis in Mice. Gastroenterology. 2015; 149:1884–95.e4. [PubMed: 26261008]
22. Michailidi C, Hayashi M, Datta S, Sen T, Zenner K, Oladeru O, Brait M, Izumchenko E, Baras A, VandenBussche C, Argos M, Bivalacqua TJ, et al. Involvement of epigenetics and EMT-related miRNA in arsenic-induced neoplastic transformation and their potential clinical use. Cancer Prev Res (Phila). 2015; 8:208–21. [PubMed: 25586904]
23. Tzeng CC, Liu HS, Li C, Jin YT, Chen RM, Yang WH, Lin JS. Characterization of two urothelium cancer cell lines derived from a blackfoot disease endemic area in Taiwan. Anticancer Res. 1996; 16:1797–804. [PubMed: 8712703]
24. Ahsan H, Chen Y, Parvez F, Argos M, Hussain AI, Momotaj H, Levy D, van Geen A, Howe G, Graziano J. Health Effects of Arsenic Longitudinal Study (HEALS): description of a multidisciplinary epidemiologic investigation. J Expo Sci Environ Epidemiol. 2006; 16:191–205. [PubMed: 16160703]
25. Sage AP, Minatel BC, Ng KW, Stewart GL, Dummer TJB, Lam WL, Martinez VD. Oncogenomic disruptions in arsenic-induced carcinogenesis. Oncotarget. 2017; 8:25736–55. [PubMed: 28179585]
26. Ooki A, Del Carmen Rodriguez Pena M, Marchionni L, Dinalankara W, Begum A, Hahn NM, VandenBussche CJ, Rasheed ZA, Mao S, Netto GJ, Sidransky D, Hoque MO. YAP1 and COX2 Coordinately Regulate Urothelial Cancer Stem-like Cells. Cancer Res. 2018; 78:168–81. [PubMed: 29180467]

Author Manuscript Author Manuscript Author Manuscript Author Manuscript

27. Mani SA, Guo W, Liao MJ, Eaton EN, Ayyanan A, Zhou AY, Brooks M, Reinhard F, Zhang CC, Shipitsin M, Campbell LL, Polyak K, et al. The epithelial-mesenchymal transition generates cells with properties of stem cells. Cell. 2008; 133:704–15. [PubMed: 18485877]
28. Pastrana E, Silva-Vargas V, Doetsch F. Eyes wide open: a critical review of sphere-formation as an assay for stem cells. Cell Stem Cell. 2011; 8:486–98. [PubMed: 21549325]
29. Mantovani A, Allavena P, Sica A, Balkwill F. Cancer-related inflammation. Nature. 2008; 454:436–44. [PubMed: 18650914]
30. Rundhaug JE, Simper MS, Surh I, Fischer SM. The role of the EP receptors for prostaglandin E2 in skin and skin cancer. Cancer Metastasis Rev. 2011; 30:465–80. [PubMed: 22012553]
31. Marchiset-Ferlay N, Savanovitch C, Sauvant-Rochat MP. What is the best biomarker to assess arsenic exposure via drinking water? Environ Int. 2012; 39:150–71. [PubMed: 22208756]
32. Choi W, Porten S, Kim S, Willis D, Plimack ER, Hoffman-Censits J, Roth B, Cheng T, Tran M, Lee IL, Melquist J, Bondaruk J, et al. Identification of distinct basal and luminal subtypes of muscle-invasive bladder cancer with different sensitivities to frontline chemotherapy. Cancer Cell. 2014; 25:152–65. [PubMed: 24525232]
33. Damrauer JS, Hoadley KA, Chism DD, Fan C, Tiganelli CJ, Wobker SE, Yeh JJ, Milowsky MI, Iyer G, Parker JS, Kim WY. Intrinsic subtypes of high-grade bladder cancer reflect the hallmarks of breast cancer biology. Proc Natl Acad Sci U S A. 2014; 111:3110–5. [PubMed: 24520177]
34. Rebouissou S, Bernard-Pierrot I, de Reynies A, Lepage ML, Krucker C, Chapeaublanc E, Herault A, Kamoun A, Caillault A, Letouze E, Elarouci N, Neuzillet Y, et al. EGFR as a potential therapeutic target for a subset of muscle-invasive bladder cancers presenting a basal-like phenotype. Sci Transl Med. 2014; 6:244ra91.
35. Weinstein J, Akbani R, Broom B, Wang W, Verhaak R, McConkey D, Lerner S, Morgan M. Comprehensive molecular characterization of urothelial bladder carcinoma. Nature. 2014; 507:315–22. [PubMed: 24476821]
36. Choi W, Czerniak B, Ochoa A, Su X, Siefker-Radtke A, Dinney C, McConkey DJ. Intrinsic basal and luminal subtypes of muscle-invasive bladder cancer. Nat Rev Urol. 2014; 11:400–10. [PubMed: 24960601]
37. Kurtova AV, Xiao J, Mo Q, Pazhanisamy S, Krasnow R, Lerner SP, Chen F, Roh TT, Lay E, Ho PL, Chan KS. Blocking PGE2-induced tumour repopulation abrogates bladder cancer chemoresistance. Nature. 2015; 517:209–13. [PubMed: 25470039]
38. Beck B, Blanpain C. Unravelling cancer stem cell potential. Nature reviews Cancer. 2013; 13:727–38. [PubMed: 24060864]
39. Sarkar A, Huebner AJ, Sulahian R, Anselmo A, Xu X, Flattery K, Desai N, Sebastian C, Yram MA, Arnold K, Rivera M, Mostoslavsky R, et al. Sox2 Suppresses Gastric Tumorigenesis in Mice. Cell Rep. 2016; 16:1929–41. [PubMed: 27498859]
40. Chang Q, Chen B, Thakur C, Lu Y, Chen F. Arsenic-induced sub-lethal stress reprograms human bronchial epithelial cells to CD61 cancer stem cells. Oncotarget. 2014; 5:1290–303. [PubMed: 24675390]
41. Chou R, Gore JL, Buckley D, Fu R, Gustafson K, Griffin JC, Grusing S, Selph S. Urinary Biomarkers for Diagnosis of Bladder Cancer: A Systematic Review and Meta-analysis. Ann Intern Med. 2015; 163:922–31. [PubMed: 26501851]
42. Zhang ML, Rosenthal DL, VandenBussche CJ. The cytomorphological features of low-grade urothelial neoplasms vary by specimen type. Cancer Cytopathol. 2016; 124:552–64. [PubMed: 27019161]
43. Kaufman DS, Shipley WU, Feldman AS. Bladder cancer. Lancet. 2009; 374:239–49. [PubMed: 19520422]
44. Pang LY, Hurst EA, Argyle DJ. Cyclooxygenase-2: A Role in Cancer Stem Cell Survival and Repopulation of Cancer Cells during Therapy. Stem Cells Int. 2016; 2016:2048731. [PubMed: 27882058]
45. Singh S, Trevino J, Bora-Singhal N, Coppola D, Haura E, Altiok S, Chellappan SP. EGFR/Src/Akt signaling modulates Sox2 expression and self-renewal of stem-like side-population cells in non-small cell lung cancer. Mol Cancer. 2012; 11:73. [PubMed: 23009336]

Author Manuscript Author Manuscript Author Manuscript Author Manuscript

46. Wang F, Liu S, Xi S, Yan L, Wang H, Song Y, Sun G. Arsenic induces the expressions of angiogenesis-related factors through PI3K and MAPK pathways in SV-HUC-1 human uroepithelial cells. Toxicol Lett. 2013; 222:303–11. [PubMed: 23968725]

47. Chen G. STAT3 in arsenic lung carcinogenicity. Oncoimmunology. 2015; 4:e995566. [PubMed: 26137408]

48. Cui X, Kobayashi Y, Akashi M, Okayasu R. Metabolism and the paradoxical effects of arsenic: carcinogenesis and anticancer. Curr Med Chem. 2008; 15:2293–304. [PubMed: 18781951]

49. Vaz M, Hwang SY, Kagiampakis I, Phallen J, Patil A, O'Hagan HM, Murphy L, Zahnow CA, Gabrielson E, Velculescu VE, Easwaran HP, Baylin SB. Chronic Cigarette Smoke-Induced Epigenomic Changes Precede Sensitization of Bronchial Epithelial Cells to Single-Step Transformation by KRAS Mutations. Cancer Cell. 2017; 32:360–76.e6. [PubMed: 28898697]

50. Dai YC, Wang SC, Haque MM, Lin WH, Lin LC, Chen CH, Liu YW. The interaction of arsenic and N-butyl-N-(4-hydroxybutyl)nitrosamine on urothelial carcinogenesis in mice. PLoS One. 2017; 12:e0186214. [PubMed: 29016672]

Author Manuscript Author Manuscript Author Manuscript Author Manuscript

Novelty and Impact

Environmental exposures to arsenic are associated with the development of urothelial carcinoma of the bladder (UCB). However, the molecular mechanisms of arsenic-induced UCB remain elusive. Here, we demonstrated that chronic arsenic exposure induced malignant stem cell transformation of immortalized human urothelial cells via the overactivation of COX2/PGE2-SOX2 axis. In addition, the expression levels of SOX2 and COX2 may have the potential as urinary markers for risk assessment of arsenic exposure and for UCB detection.

Author Manuscript Author Manuscript Author Manuscript Author Manuscript

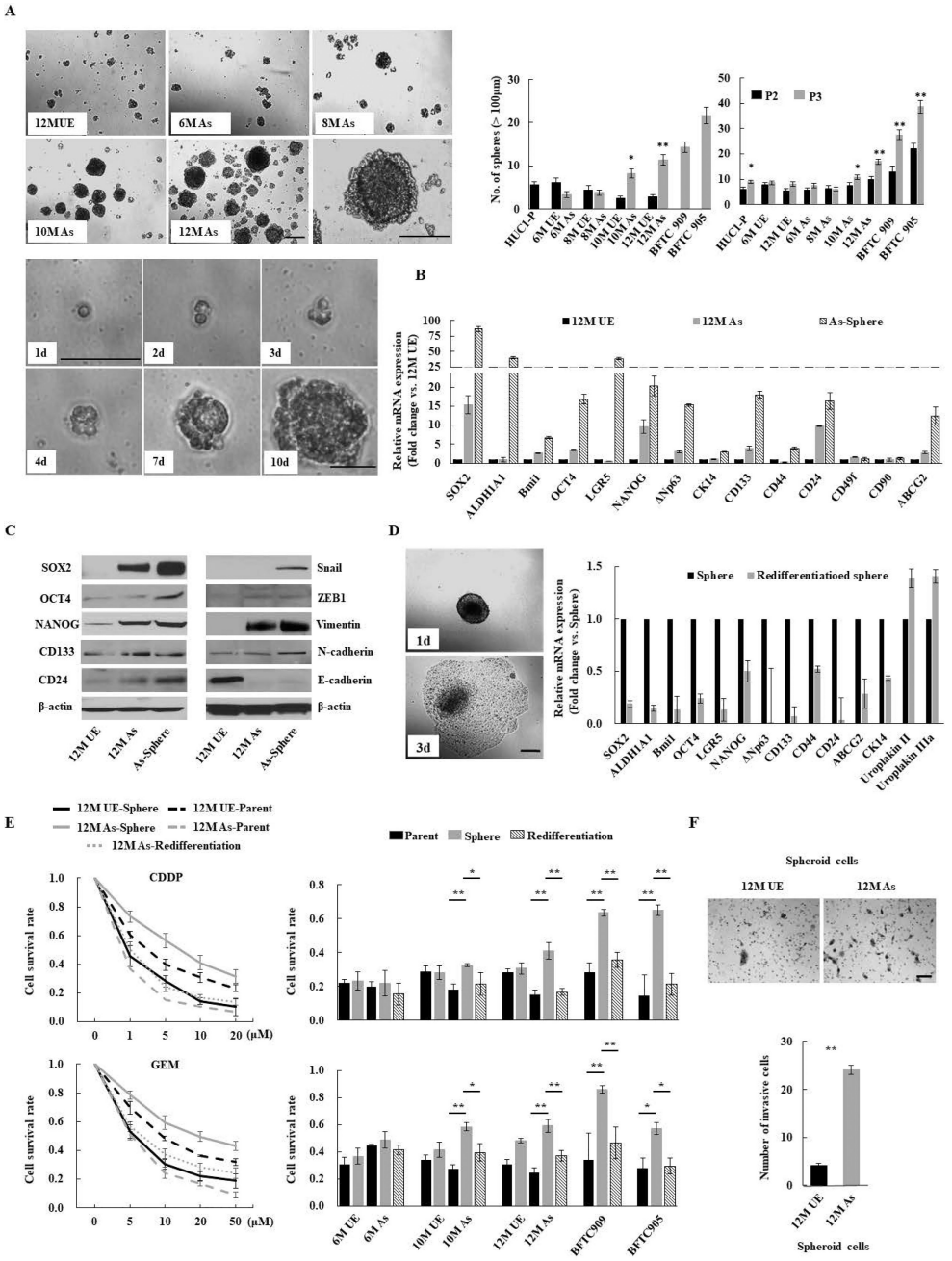

Figure 1.

Chronic arsenic exposure-induced malignant stemness properties in immortalized human urothelial cells (HUC1). (**A**) Sphere formation and self-renewal assays in chronic arsenic-exposed (As)-cells for 6 to 12 months (6M As- to 12M As-cells) compared with the passage-matched unexposed (UE)-cells. Upper left: representative images of spheres according to different time periods of arsenic exposure (scale bars, 200 μm); Lower left: representative consecutive images of secondary sphere formed from single spheroid 12M-As cell (scale bars, 200 μm). Right: the number of spheres over 100 μm; left bar graph: the number of spheres in As-cells and UE-cells; right bar graph: the number of spheroid cells after second

Author Manuscript Author Manuscript Author Manuscript Author Manuscript

(P2) and third (P3) passage in self-renewal assay. Data are from 3 independent experiments. BFTC 905 and 909 cell lines, established from arsenic exposed UCB subjects, were used as controls. (**B**) Relative expression of stemness-related molecules using Q-RT-PCR in parental or spheroid As-cells compared with UE-cells. (**C**) Western blotting of stem cell- and EMT-related molecules. (**D**) Spheroid As-cells-induced re-differentiation. When spheroid cells were cultured under standard conditions containing FBS, the floating spheroid cells could adhere and acquire epithelial morphology similar to parental cells (scale bars, 200 μm; left). The cells showed higher differentiation markers such as uroplakin II or IIIA, and lower stem cell markers compared with corresponding spheroid cells, as measured by Q-RT-PCR (right), indicating re-differentiation. (**E**) Chemo-resistance property of Spheroid As-cells. Left: cell viability determined by MTT assay after various concentrations of CDDP or GEM treatment for 72 hours in indicated cells. The ratio of absorbance values of various concentrations treatment related to the value of mock was considered as 1.0. Right: cell viability after 10 μM CDDP or GEM treatment of As-cells exposed at different time periods of arsenic. Spheroid cells were cultured in ultra-low attachment 96 well plates under serum-free condition. Spheroid As-cells were significantly more chemo-resistant than parental As- and re-differentiated cells. (**F**) Invasion assay of spheroid As-cells. Upper: representative images (scale bars, 100 μm); Lower: the number of invaded cells. Spheroid As-cells were a more invasive phenotype than spheroid UE-cells. Each error bar indicates mean ± SEM. * P <0.05, ** P <0.01 [Wilcoxon-Mann-Whitney test (A and F) and Kruskal-Wallis with post-hoc test (E)].

Author Manuscript
Author Manuscript
Author Manuscript
Author Manuscript

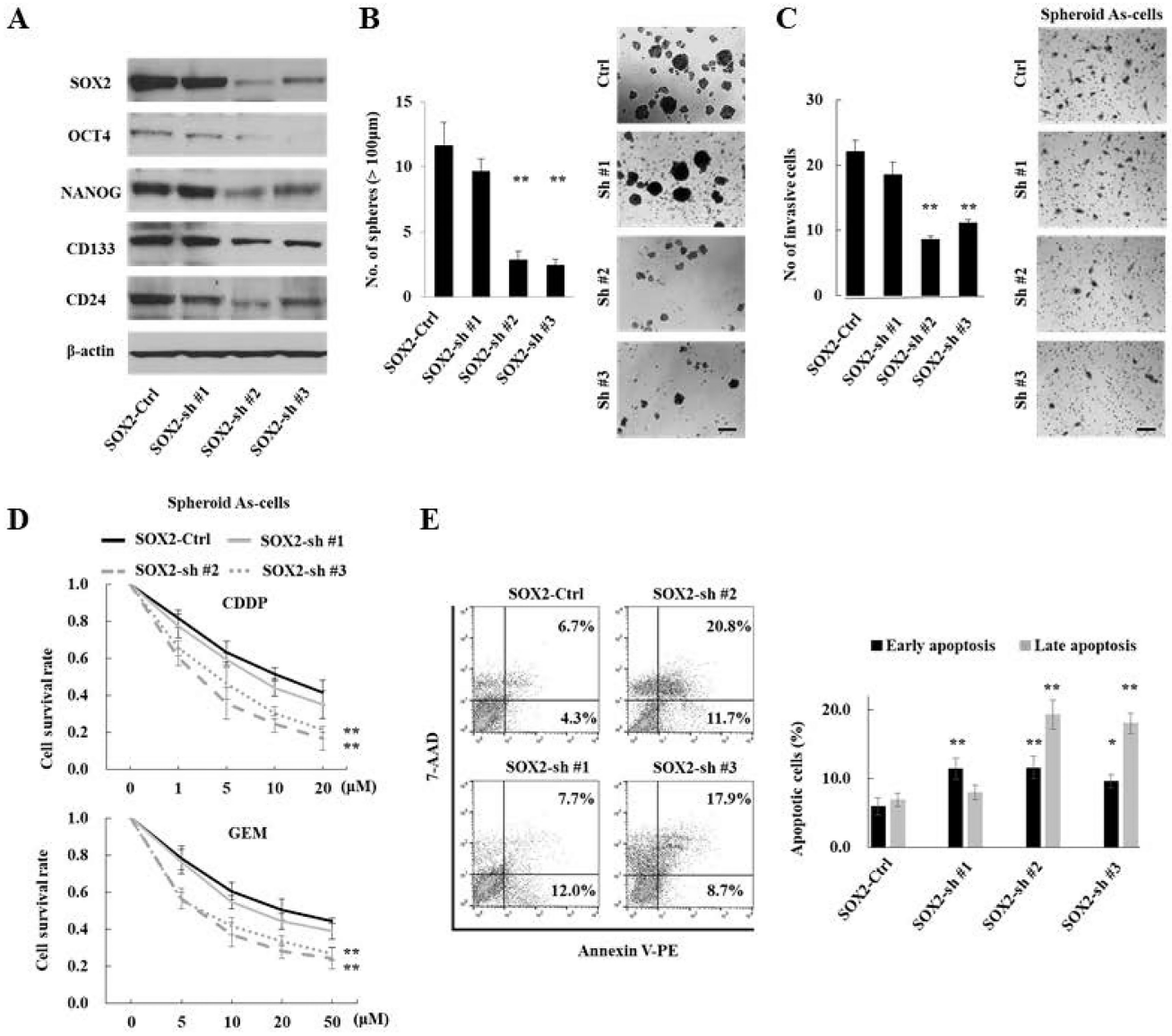

Figure 2.

SOX2 is a critical oncogene and linked to arsenic-induced malignant stemness properties. (**A**) Western blotting analysis of stemness-related molecules in 12M As-cells transduced with SOX2 shRNA (SOX2-sh cells) or control shRNA (SOX2-Ctrl cells). SOX2 knockdown repressed expression of OCT4, NANOG, CD133, and CD24. (**B**) Sphere formation assay in SOX2-sh cells. SOX2 knockdown attenuated sphere forming ability. Left: the number of spheres over 100 μm; Right: representative images (scale bars, 200 μm). (**C**) Invasion assay of spheroid SOX2-sh cells. Left: the number of invaded cells; Right: representative images (scale bars, 100 μm). (**D**) Cell viability after 10μM CDDP (upper) or GEM (lower) treatment for 72 hours in spheroid SOX2-sh cells. (**E**) Apoptosis assay: 72 hours after treatment with CDDP (10 μM) in spheroid SOX2-sh cells. Left: representative image of late apoptosis (top right quadrant) and early apoptosis (bottom right quadrant); Right: the number of apoptotic cells. Spheroid SOX2-sh cells were more sensitive to apoptosis against CDDP treatment.

Author Manuscript Author Manuscript Author Manuscript Author Manuscript

Each error bar indicates mean ± SEM. * $P<0.05$, ** $P<0.01$ (Wilcoxon-Mann-Whitney test).

Author Manuscript
Author Manuscript
Author Manuscript
Author Manuscript

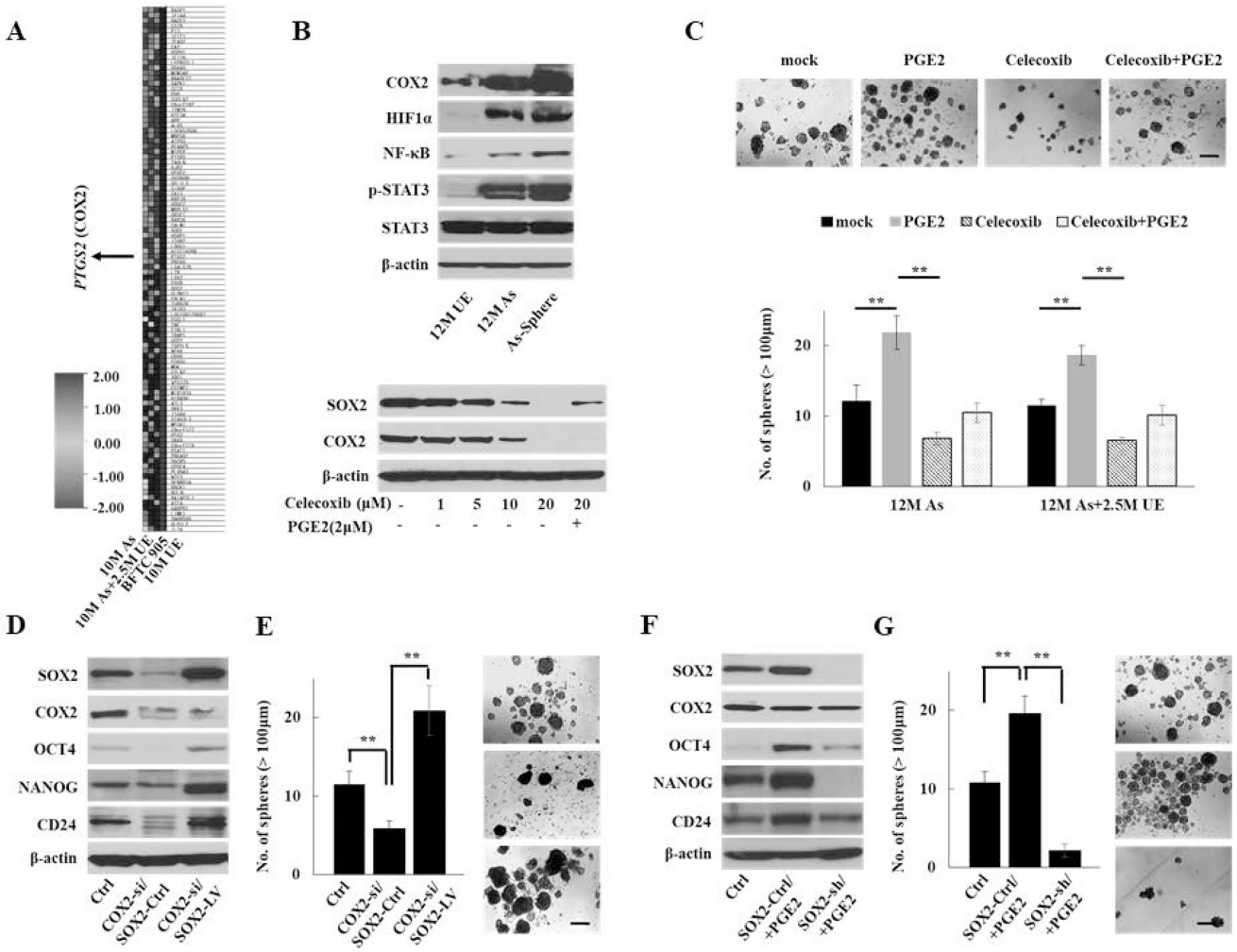

Figure 3.

COX2/PGE2-SOX2 axis in maintaining malignant stem cells. (**A**) Heat map of top 50 genes with the most enriched score determined by GSEA for the oncogenic signatures on 10M As-cells, 10M As-cells cultured without arsenic for 2.5 months (10M As+2.5M UE-cells), and BFTC905 cells compared with 10M UE-cells. PTGS2 (encoding COX2) was one of the top 50 genes with the most enriched score. (**B**) Western blotting of inflammation-related molecules, including COX2 in parental or spheroid As-cells compared with UE-cells (upper) and dynamics of SOX2 and COX2 expression after treatment with COX2 inhibitor celecoxib for 72 hours ± PGE2 (2 μM) for 24 hours in As-cells (lower). (**C**) Sphere formation assay in 12 M As-cells or 12M As-cells that were cultured for 2.5M without arsenic (12M As+2.5M UE) treated with celecoxib (10 μM) and/or PGE2 (2 μM) for 72 hours. Upper: representative images (scale bars, 200 μm). Lower: Bar graph of number of spheres of indicated cell lines. Data are from 3 independent experiments. (**D**) Western blotting of SOX2, COX2, and stemenss-related molecules after forced expression of SOX2 in COX2 knockdown As-cells. (**E**) Sphere formation assay after forced expression of SOX2 in COX2 knockdown 12M As-cells (scale bars, 200 μm). (**F**) Western blotting of SOX2, COX2, and stemenss-related molecules after knockdown of SOX2 in 12M As-cells treated with PGE2. (**G**) Sphere

formation assay after knockdown of SOX2 in 12M As-cells treated with PGE2 (scale bars, 200 μm). Each error bar indicates mean ± SEM. * $P<0.05$, ** $P<0.01$ [Kruskal-Wallis with post-hoc test (C, E, and G)].

Author Manuscript Author Manuscript Author Manuscript Author Manuscript

Author Manuscript Author Manuscript Author Manuscript Author Manuscript

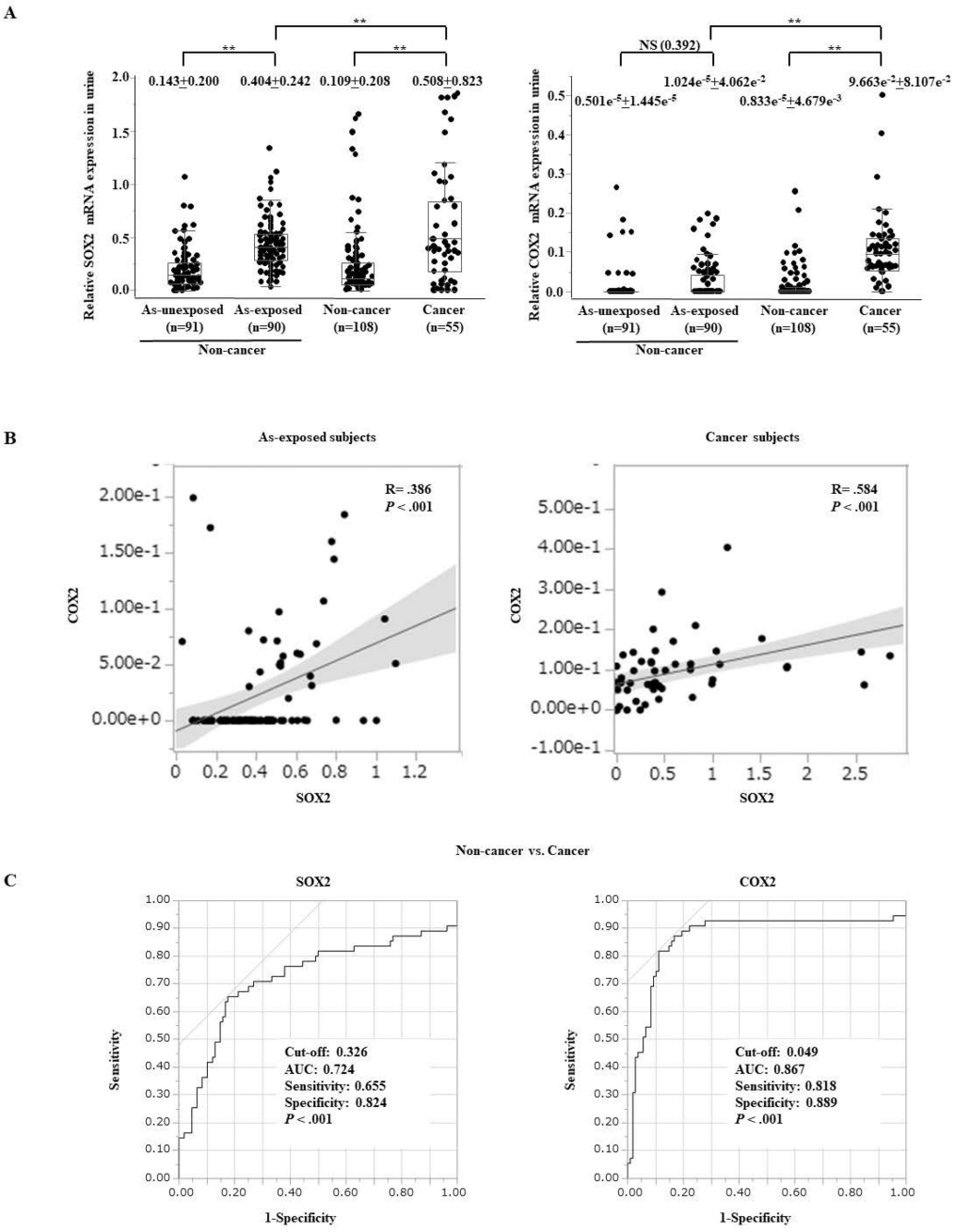

Figure 4.

Elevated expression of SOX2 and COX2 in urine samples from non-cancer arsenic exposed and UCB subjects compared with controls. (**A**) Box plots of SOX2 (left) and COX2 (right) expression measured by Q-RT-PCR in urine from arsenic (As)-unexposed (n=91) and exposed (n=90) non-cancer subjects; and from UCB (n=55) and population-matched control subjects (n=108). The median ± interquartile range is shown. NS, not significant; ** $P <$ 0.01 (Kruskal-Wallis with post-hoc test). (**B**) A linear correlation analysis between mRNA expression status of SOX2 and COX2 in arsenic (As)-exposed subjects (left) and in UCB subjects (right) using Pearson product-moment. (**C**) A receiver operating characteristic curve

(ROC) analysis of SOX2 (left) and COX2 (right) for non-invasive cancer detection using urine samples from 55 UCB subjects and 108 population-matched control subjects.

Author Manuscript Author Manuscript Author Manuscript Author Manuscript

Author Manuscript Author Manuscript Author Manuscript Author Manuscript

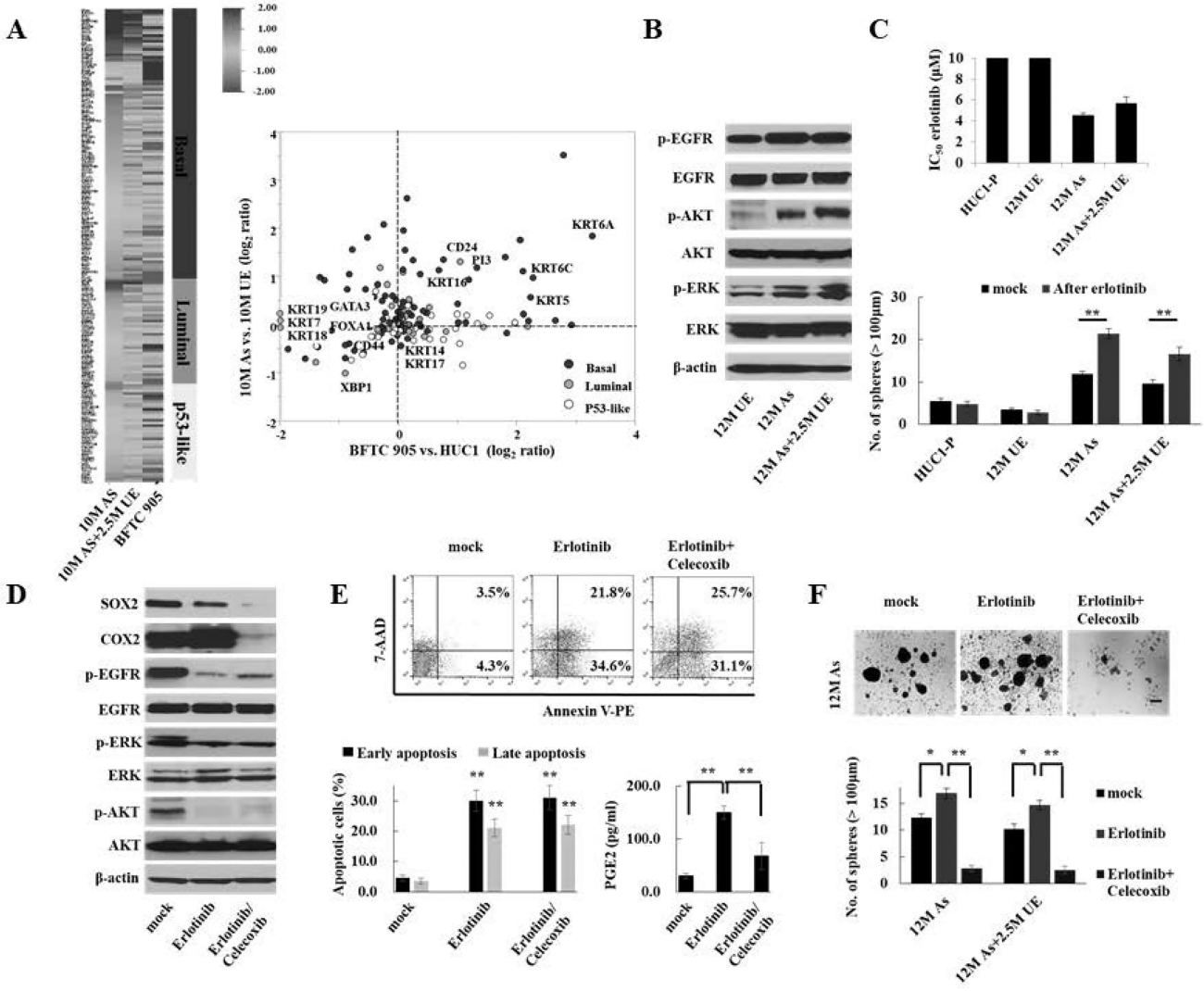

Figure 5.

COX2/PGE2-SOX2 axis-induced stem cell enrichment following EGFR-targeted therapy in As-cells exhibiting a basal-type signature. (**A**) Arsenic-induced basal-type gene signature: Left, heat map of gene expression pattern according to the molecular subtypes in 10M As-cells, 10M As+2.5M UE, and BFTC905 (basal-type) cells compared with 10M UE-cells. Right: Scatter plot of representative genes in different molecular subtypes of UCB. As-cells showed basal-type signature. The gene expression profiles according to the molecular subtypes are shown in Supplemental Table 5. (**B**) Western blotting of selected EGFR pathway genes in As-cells. Chronic arsenic-exposure activated EGFR pathway, including downstream AKT and ERK signaling. (**C**) The half-maximal inhibitory concentration (IC_{50}) value of the EGFR inhibitor erlotinib (upper) and sphere formation assay after treatment with 1 μM of erlotinib (lower) for 72 hours in As-cells exhibiting a basal-type signature. The IC_{50} value was calculated by exposing the cells to the various concentrations of erlotinib for 72 hours using a MTT assay. (**D**) Dynamics of the SOX2 and COX2 expression after treatment with 1 μM of erlotinib ± 10 μM of celecoxib for 72 hours in As-cells. Dual inhibition of EGFR and COX2 dramatically decreased SOX2 expression compared with

Author Manuscript Author Manuscript Author Manuscript Author Manuscript

EGFR inhibition alone. (**E**) Apoptosis assay and ELISA assay of PGE2 after treatment with 1 μM erlotinib ± 10 μM celecoxib for 72 hours in As-cells. Data are from 3 independent experiments. Upper: representative image of early apoptosis (bottom right quadrant) and late apoptosis (top right quadrant); Lower left: percentage of apoptotic cells; Lower right: ELISA assay of PGE2. As-cells were more susceptible to apoptosis against treatment with erlotinib, resulting in an increased production of PGE2. Addition of celecoxib treatment attenuated PGE2 production due to apoptosis. (**F**) Sphere formation assay after treatment with 1 μM erlotinib ± 10 μM celecoxib for 72 hours in As-cells and As+2.5M UE-cells. Upper: representative images (scale bars, 200 μm); Lower: the number of spheres. Each error bar indicates mean ± SEM. * $P<0.05$, ** $P<0.01$ [Wilcoxon-Mann-Whitney test (lower left in E) and Kruskal-Wallis with post-hoc test (C, lower right in E, and F)].